Mechanical Tough yet Self-Healing Transparent Conductive Elastomers through Synergic Dual Cross-Linking Strategy

Qiankun Zhang, Guangxue Chen, Ren'ai Li, Liang Lin and Minghui He**

State Key Laboratory of Pulp and Paper Engineering, School of Light Industry and Engineering, South China University of Technology, Guangzhou 510640, China.

Table S1. General Formula for the classification of deep eutectic solvents[1, 2]

type	general formula	terms
type Ⅰ	Cat^+X^-zMClx	M = Zn, Sn, Fe, Al, Ga, In
type Ⅱ	$Cat^+X^-zMCl_x{\cdot}yH_2O$	M = Cr, Co, Cu, Ni, Fe
type Ⅲ	Cat^+X^-zRZ	Z = $CONH_2$, COOH, OH
type Ⅳ	$MCl_x + RZ = MCl_{x-1}^+{\cdot}RZ + MCl_{x+1}^-$	M = Al, Zn and Z = $CONH_2$, OH

Deep eutectic solvents can be described by the general formula:

$$Cat^+X^-zY \quad (1)$$

where Cat^+ is in principle any ammonium, phosphonium, or sulfonium cation, and X is a Lewis base, generally a halide anion. The complex anionic species are formed between X^- and either a Lewis or Brønsted acid Y (z refers to the number of Y molecules that interact with the anion).

Table S2. The detailed components and mole ratios of the prepared PDESs

Sample	ChCl:AA: $AlCl_3{\cdot}6H_2O$ (mole ratio)	Appearance
PDES-0	1:2:0	Transparent, colorless liquid
PDES-1/100	1:2:1/100	Transparent, colorless liquid
PDES-1/50	1:2:1/50	Transparent, colorless liquid
PDES-1/25	1:2:1/25	Transparent, colorless liquid
PDES-1/5	1:2:1/5	turbid liquid with precipitation

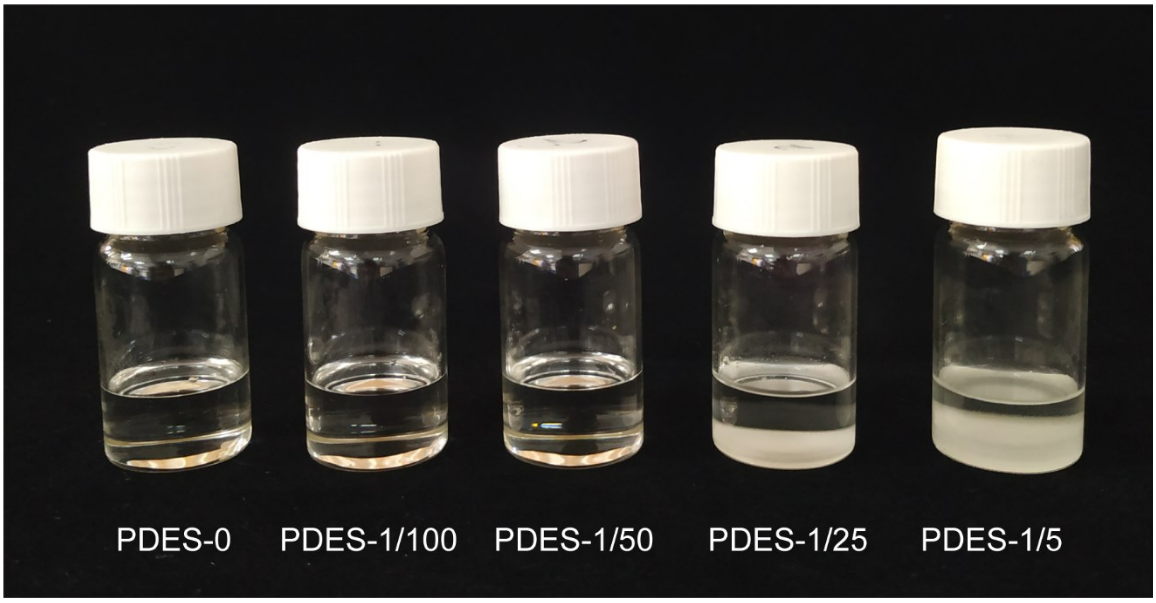

Figure S1. The physical appearances of ChCl, AA, and $AlCl_3 \cdot 6H_2O$ mixtures with various mole ratios.

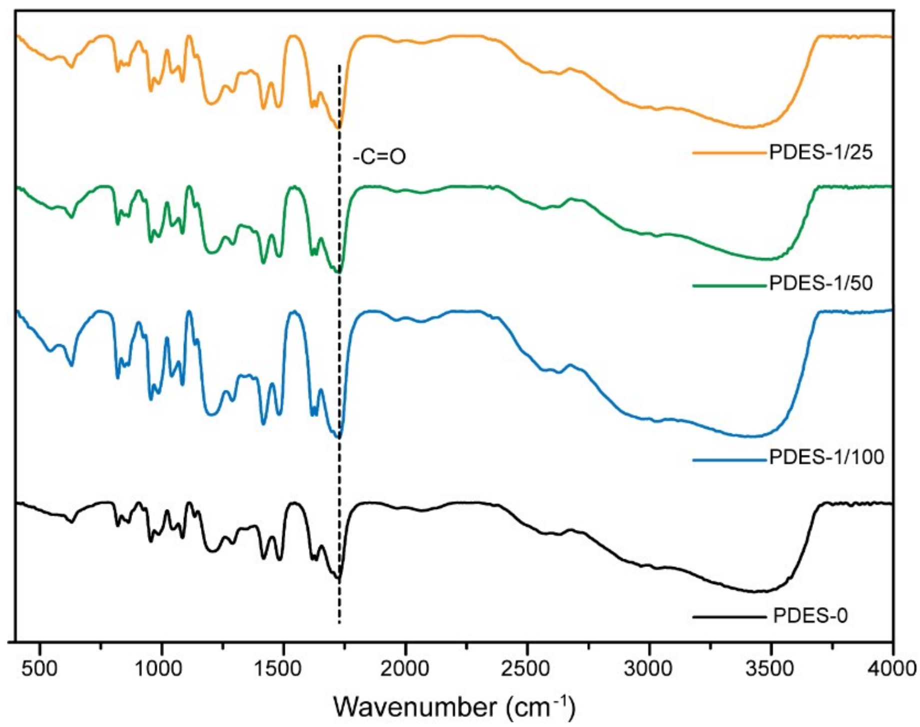

Figure S2. FTIR spectroscopy of PDESs with various Al(III) content

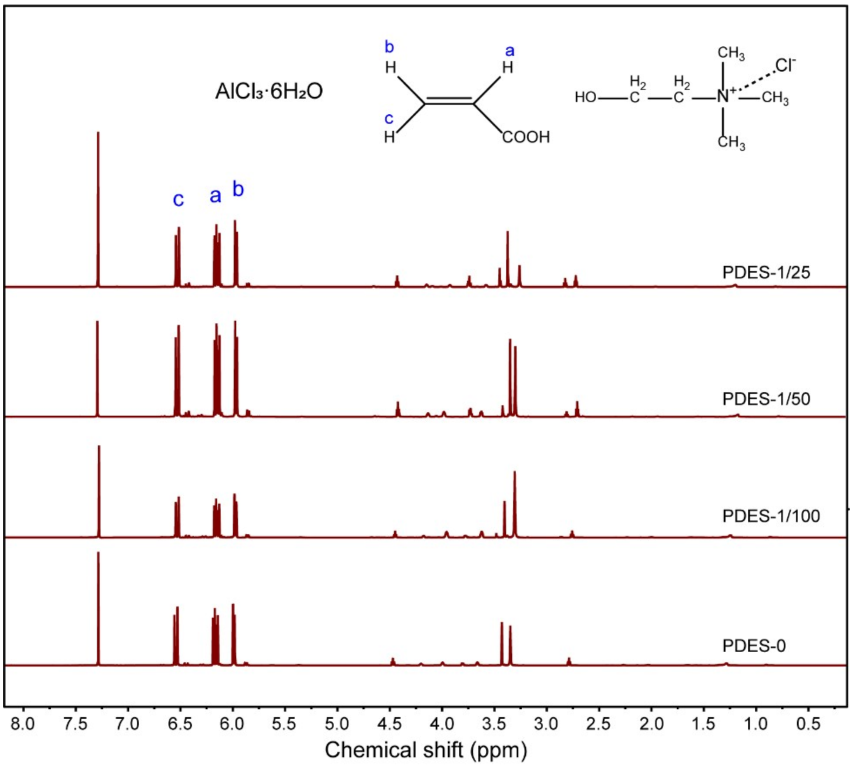

Figure S3. [1]H NMR spectra of ChCl/AA/Al(III) type PDESs. The spectra were recorded using $CDCl_3$ as the external reference.

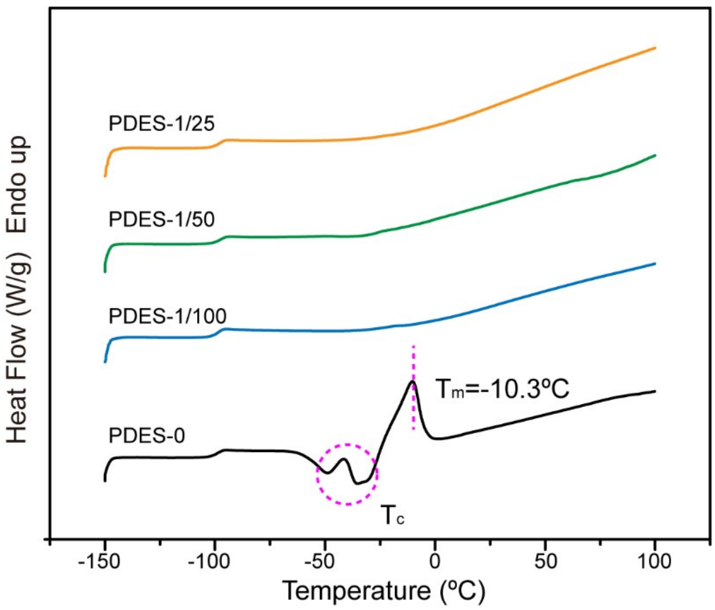

Figure S4. DSC traces for PDESs with various Al(III) content.

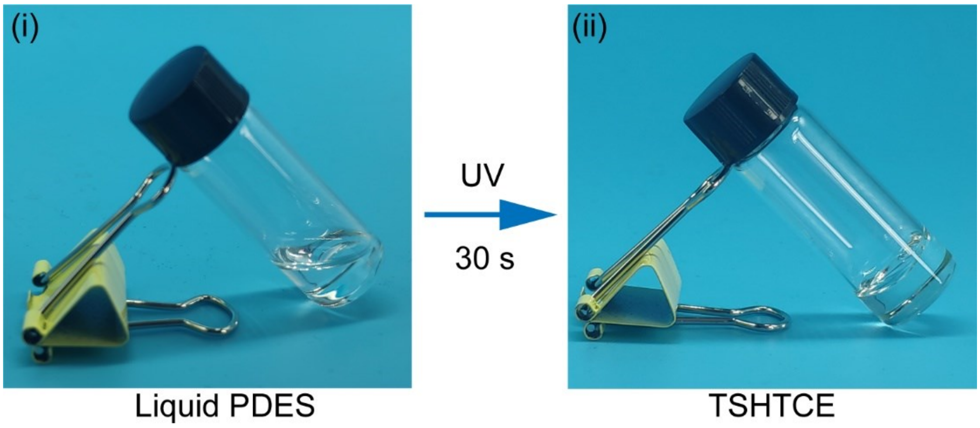

Figure S5. Digital photographs of PDES before (i) and after (ii) photopolymerization.

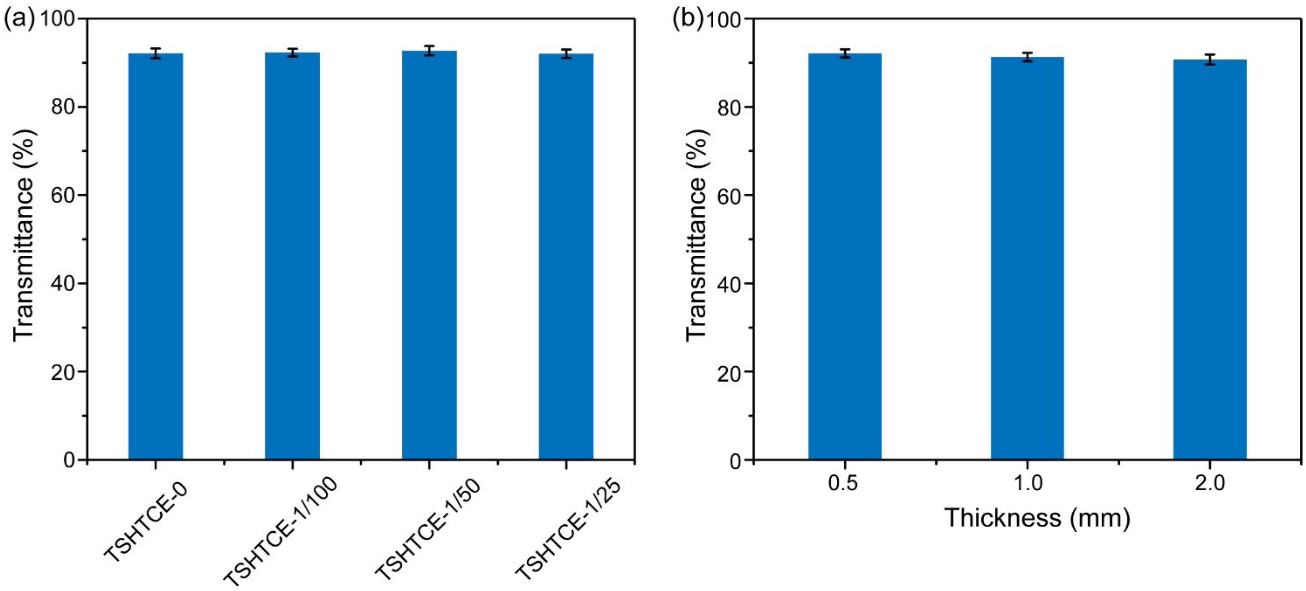

Figure S6. Optical transmittance of TSHTCEs with various (a) Al(III) content and (b) thickness.

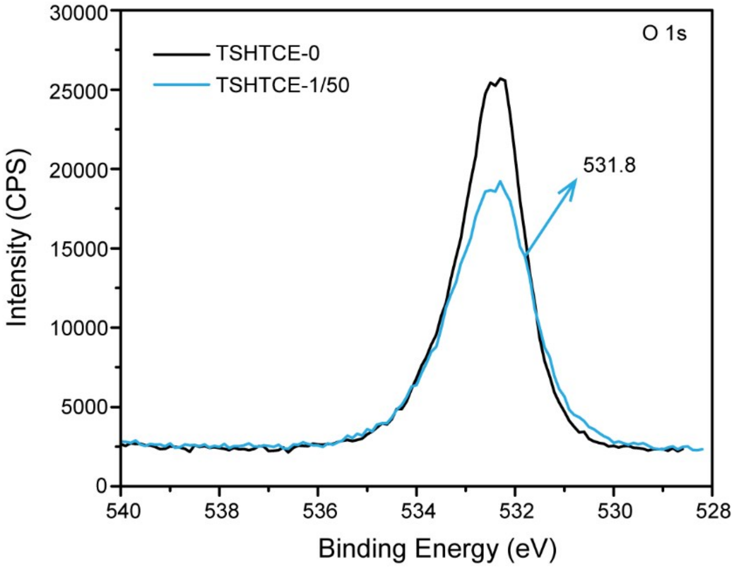

Figure S7. The high-resolution O 1s peak for TSHTCE-0 and TSHTCE-1/50. As shown, a new peak occurred at 531.8 eV, which can be ascribed to Al(III)-carboxyl complexes.

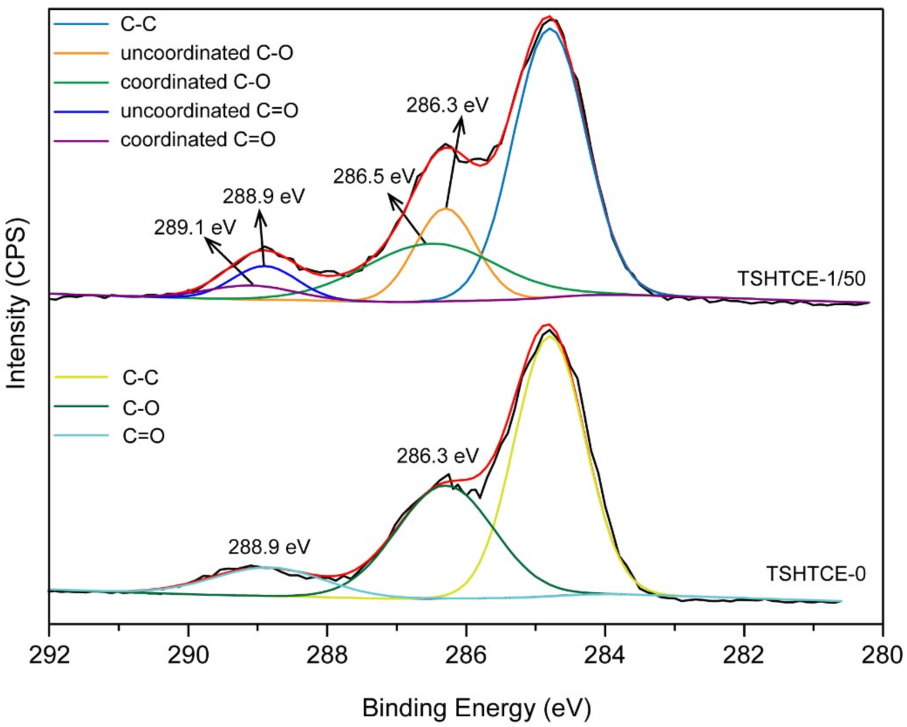

Figure S8. C1s peak for TSHTCE-0 (down) and TSHTCE-1/50 (top).

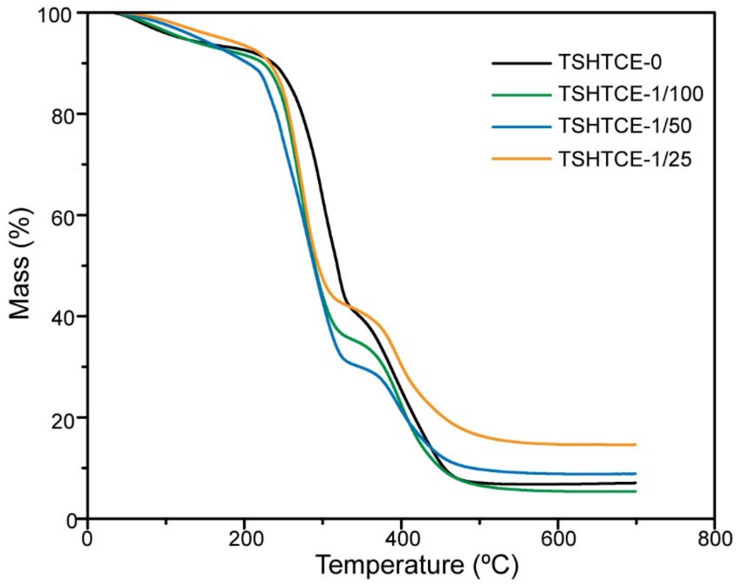

Figure S9. Thermal gravimetric analysis (TGA) curves of TSHTCEs with various Al(III) content.

Figure S10. A TSHTCE film can lift a 1500 g load without significant elongation, which is 1000 times greater than its own weight.

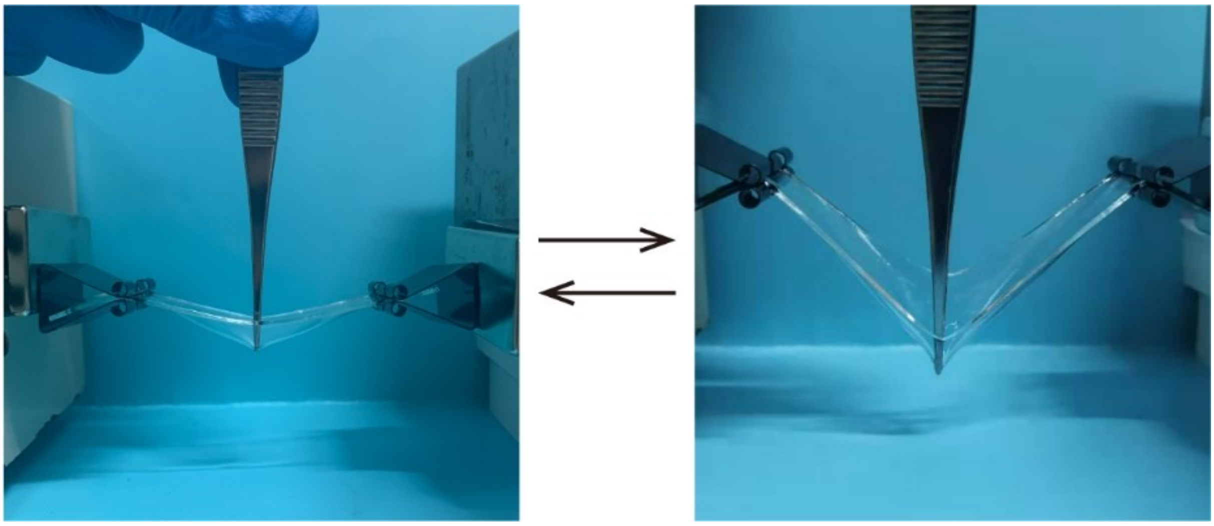

Figure S11. The TSHTCE film exhibit excellent puncture-resistance capability.

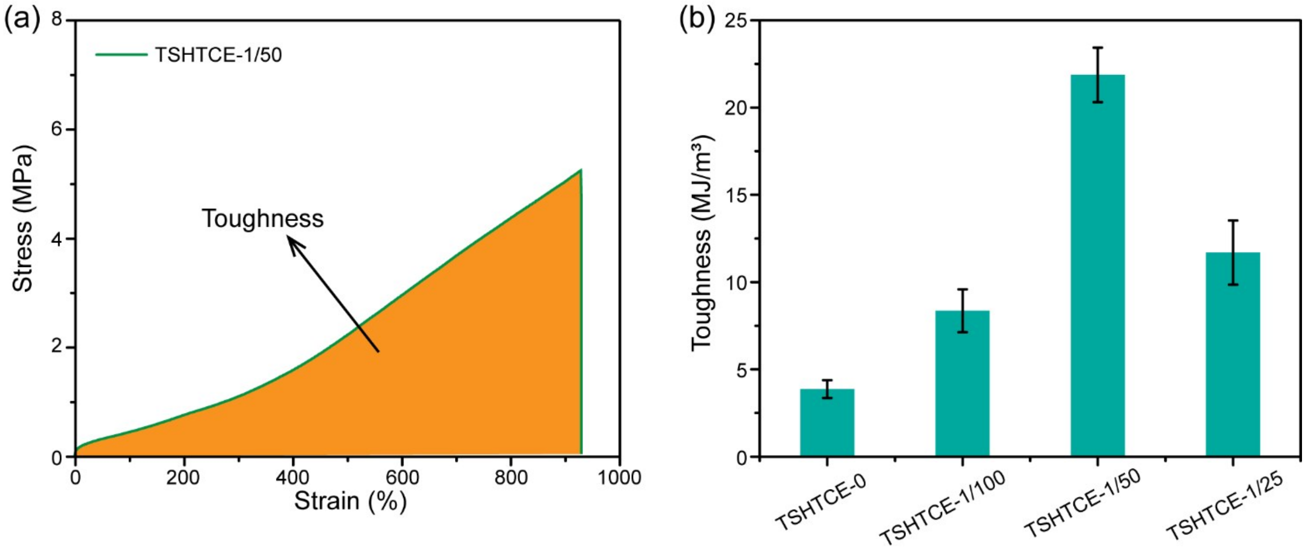

Figure S12. (a) The calculation method for toughness and (b) the toughness of prepared TSHTCEs.

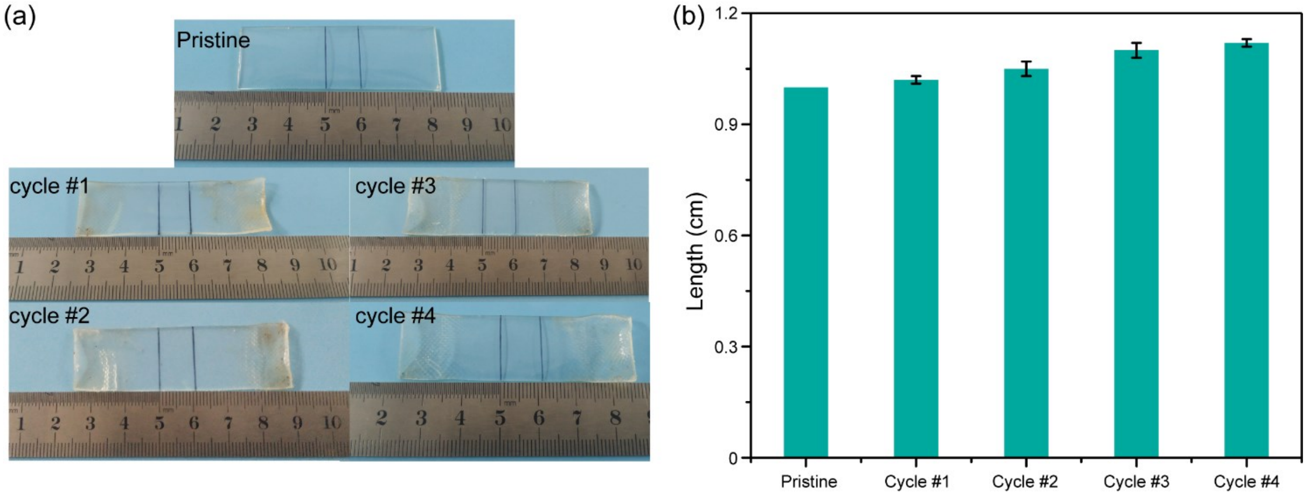

Figure S13. (a) The optical pictures and (b) measured length of TSHTCEs before and after tensile tests.

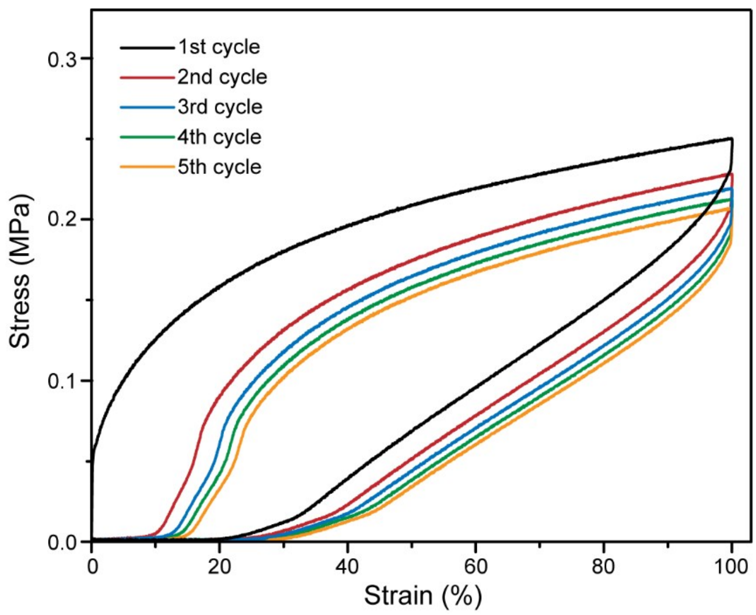

Figure S14. Cyclic tensile tests for TSHTCE-0 without Al(III) crosslinking.

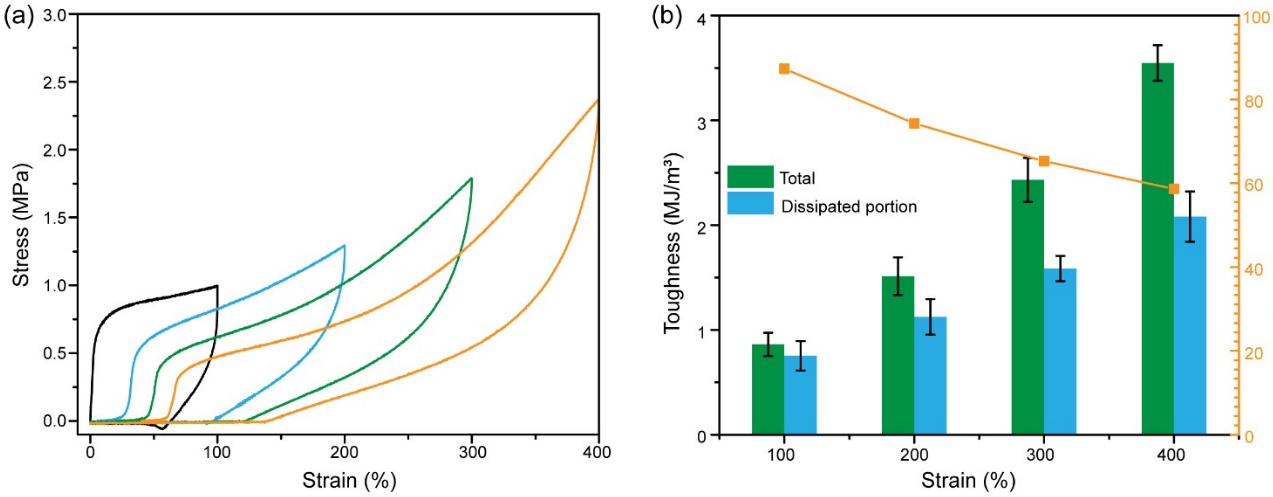

Figure S15. (a) Continuous cyclic tensile loading−unloading curves under different strains (100%, 200%, 300%, 400%) and (b) corresponding toughness and energy dissipation ratio.

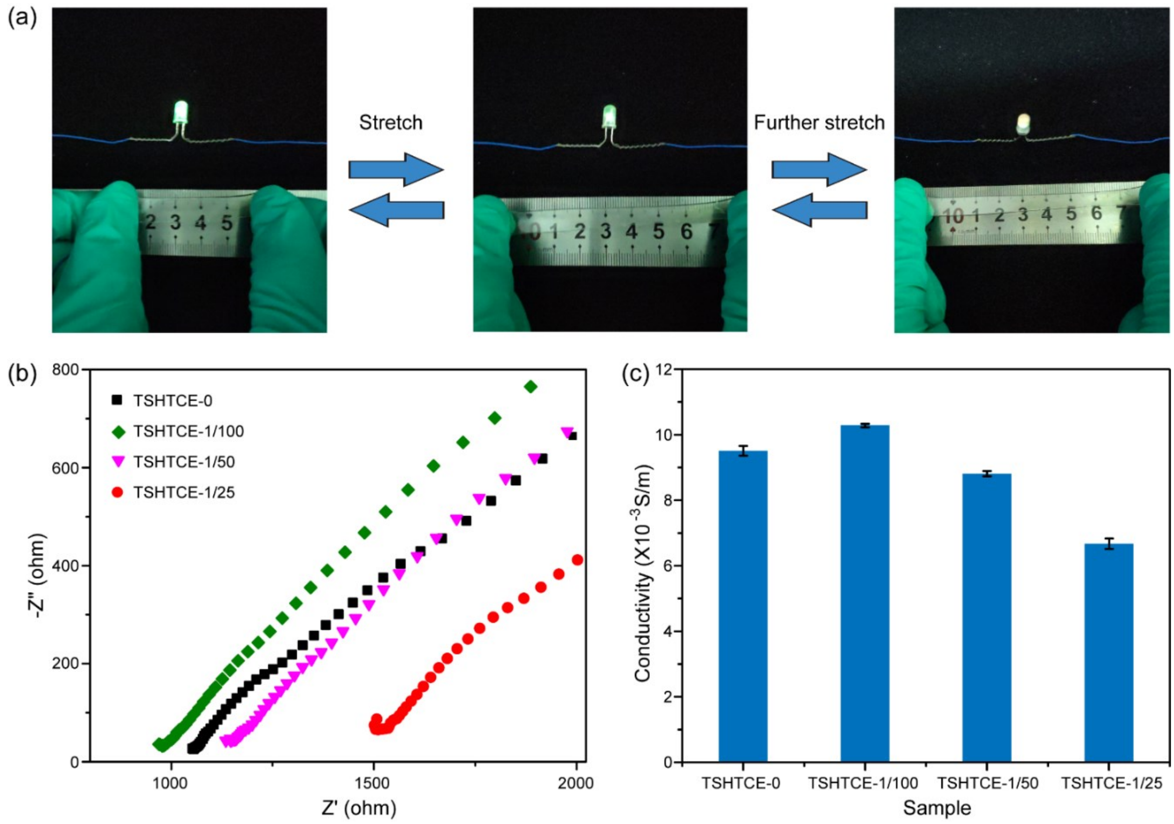

Figure S16. Electrical properties of TSHTCEs. (a) Optical diagram of a TSHTCE film in series circuit with a LED bulb, where the brightness of the LED changes with the deformation of the TSHTCE film. (b) Electrochemical impedance spectroscopy (EIS) plots and (c) the calculated ionic conductivities of TSHTCEs with various Al(III) content.

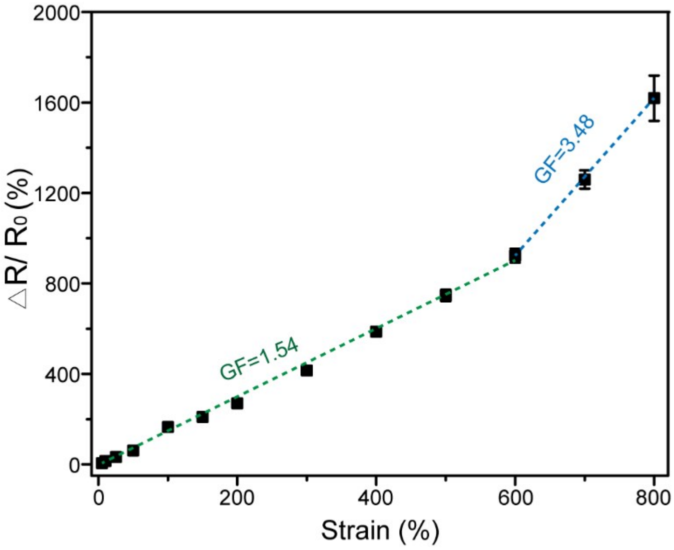

Figure S17. The dependence of relative resistance changes of TSHTCE-1/50 film on the strain.

Table S3. Comparison with existing reported polymer-based sensors

category	Components	Transparency	Conductivity	Stretchability	Mechanical strength	Self-healing	Ref.
Hydrogel	polyvinyl alcohol+ polyacrylamide	>90%	Not given	~500%	80-200 KPa	No	[3]
	poly(acrylamide-co-2-acrylamido-2-methyl-1-propanesulfonic acid)	>90%	No	~900%	~6 MPa	No	[4]
	poly(glycerol sebacate)-co-poly(ethylene glycol)-g-catechol prepolymer (PEGSD) +UPy-hexamethylene diisocyanate (HDI) synthon modified gelatin (GTU)	No	No	~1000%	2-5 KPa	Yes	[5]
	Poly(sulfobetaine methacrylate) + dopamine	~90%	Not given	~700%	30 KPa	Yes	[6]
	PDA–clay–PSBMA	No	0.02 $S \cdot m^{-1}$	~900%	80 KPa	Yes	[7]
Ionic gel	4-acryloylmorpholine + propylene carbonate	93%	7.9×10^{-4} $S \cdot cm^{-1}$	1219%	25-50 kPa	No	[8]
	1-vinyl-3-(carboxymethyl)-imidazolium+ polyacrylamide + KCl	92%	1.1 $S \cdot m^{-1}$	900%	20-60 kPa	Yes	[9]
	(LiTFSI) + butyl acrylate	92.4%	1.27×10^{-7} $S \cdot cm^{-1}$	1100%	0.25 MPa	No	[10]
	1-butyl-2,3-dimethylimidazolium	90%	10^{-5}-10^{-3} $S \cdot cm^{-1}$	1312%	0.4 MPa	No	[11]

	bis(trifluoromethylsulfonyl)amine +						
	ionic liquids+PVDFco-HFP-5545	90%	10^{-4} S cm^{-1}	5000%	0.1 MPa	No	12
This work	ChCl+AA+$AlCl_3 \cdot 6H_2O$	92%	6.64~10.29×10^{-4} S/m	470%~900%	1.28~6.03 MPa	Yes	

Reference

1. Mota Morales, J. D.; Sánchez Leija, R. J.; Carranza, A.; Pojman, J. A.; Monte, F. d.; Luna Barcenas, G. Free-radical polymerizations of and in deep eutectic solvents: Green synthesis of functional materials. *Progress in Polymer Science* **2017,** 78 (2018), 139-153.
2. Smith, E. L.; Abbott, A. P.; Ryder, K. S. Deep Eutectic Solvents (DESs) and Their Applications. *Chemical Reviews* **2014,** 114 (21), 11060-11082 DOI: 10.1021/cr300162p.
3. Ge, G.; Zhang, Y.; Shao, J.; Wang, W.; Si, W.; Huang, W.; Dong, X. Stretchable, Transparent, and Self-Patterned Hydrogel-Based Pressure Sensor for Human Motions Detection. *Advanced Functional Materials* **2018,** 28 (32), 1802576 DOI: 10.1002/adfm.201802576.
4. Yu, H. C.; Zheng, S. Y.; Fang, L.; Ying, Z.; Du, M.; Wang, J.; Ren, K.-F.; Wu, Z. L.; Zheng, Q. Reversibly Transforming a Highly Swollen Polyelectrolyte Hydrogel to an Extremely Tough One and its Application as a Tubular Grasper. *Advanced Materials* **2020,** n/a (n/a), 2005171 DOI: https://doi.org/10.1002/adma.202005171.
5. Zhao, X.; Liang, Y.; Huang, Y.; He, J.; Han, Y.; Guo, B. Physical Double-Network Hydrogel Adhesives with Rapid Shape Adaptability, Fast Self-Healing, Antioxidant and NIR/pH Stimulus-Responsiveness for Multidrug-Resistant Bacterial Infection and Removable Wound Dressing. *Advanced Functional Materials* **2020,** 30 (17), 1910748 DOI: 10.1002/adfm.201910748.
6. Zhang, C.; Zhou, Y.; Han, H.; Zheng, H.; Xu, W.; Wang, Z. Dopamine-Triggered Hydrogels with High Transparency, Self-Adhesion, and Thermoresponse as Skinlike Sensors. *ACS Nano* **2021**, DOI: 10.1021/acsnano.0c09577.
7. Pei, X.; Zhang, H.; Zhou, Y.; Zhou, L.; Fu, J. Stretchable, self-healing and tissue-adhesive zwitterionic hydrogels as strain sensors for wireless monitoring of organ motions. *Materials Horizons* **2020,** 7 (7), 1872-1882 DOI: 10.1039/D0MH00361A.
8. Gao, Y.; Shi, L.; Lu, S.; Zhu, T.; Da, X.; Li, Y.; Bu, H.; Gao, G.; Ding, S. Highly Stretchable Organogel Ionic Conductors with Extreme-Temperature Tolerance. *Chemistry of Materials* **2019,** 31 (9), 3257-3264 DOI: 10.1021/acs.chemmater.9b00170.
9. Liu, Z.; Wang, Y.; Ren, Y.; Jin, G.; Zhang, C.; Chen, W.; Yan, F. Poly(ionic liquid) hydrogel-based anti-freezing ionic skin for a soft robotic gripper. *Materials Horizons* **2020,** 7 (3), 919-927 DOI: 10.1039/C9MH01688K.
10. Shi, L.; Zhu, T.; Gao, G.; Zhang, X.; Wei, W.; Liu, W.; Ding, S. Highly stretchable and transparent ionic conducting elastomers. *Nature Communications* **2018,** 9 (1), 2630 DOI: 10.1038/s41467-018-05165-w.
11. Shi, L.; Jia, K.; Gao, Y.; Yang, H.; Ma, Y.; Lu, S.; Gao, G.; Bu, H.; Lu, T.; Ding, S. Highly Stretchable and Transparent Ionic Conductor with Novel Hydrophobicity and Extreme-Temperature Tolerance. *Research* **2020,** 2020, 2505619 DOI: 10.34133/2020/2505619.
12. Cao, Y.; Morrissey, T. G.; Acome, E.; Allec, S. I.; Wong, B. M.; Keplinger, C.; Wang, C. A Transparent, Self‐Healing, Highly Stretchable Ionic Conductor. *Advanced Materials* **2017,** 29 (10), 1605099.